Fuzzy Logic Method Use in F/A-18 Aircraft Model Identification

Gabriel Kouba,* Ruxandra Mihaela Botez,† and Nicolas Boely‡
École de Technologie Supérieure, Montréal, Quebec H3C 1K3, Canada

A mathematical model for controlling the structural deflections of an F/A-18 modified aircraft was determined in the Active Aeroelastic Wing technology program. Five sets of signals from flight flutter tests corresponding to the excited inputs (differential ailerons, collective ailerons, collective stabilizers, differential stabilizers, and rudders) were measured at the NASA Dryden Flight Research Center. Two types of signals were used to build this new model: control deflections (the inputs) and structural deflections (the outputs). The fuzzy logic method was used in identifying the nonlinear aircraft models for 16 flight-test cases, based on Mach numbers (between 0.85 and 1.30) and altitudes (between 5000 and 25,000 ft). To find the best model, we tested a variety of systems with different numbers of inputs or fuzzy logic methods. By comparing the results obtained, we conclude that the best results, in terms of our preestablished specifications, were obtained for the 12-input Sugeno system.

Nomenclature

A, D	=	two-dimensional matrices containing linear coefficient combinations between multiple inputs and multiple outputs
F	=	fuzzification function used in the Sugeno and in the Mandani-type methods
F'	=	defuzzification function used in the Sugeno and in the Mandani-type methods
N	=	number of rules and $i \in [1, \ldots, N]$
n	=	number of inputs and $j \in [1, \ldots, n]$
x, y	=	matrices containing input and output data
W	=	matrix containing each input's data weight
Z	=	matrix containing the output level (definition in Sec. III.B) for the Sugeno-type method

I. Introduction

THE work presented in this paper uses flight flutter test data obtained from the Active Aeroelastic Wing (AAW) technology research program [1–3] conducted at the NASA Dryden Flight Research Center. The aim of the AAW Technology Flight Research Program, initiated in 1996, was to validate an aircraft concept in which a lighter, more flexible, wing could be used to improve the roll performance of the F/A-18 by minimizing the maneuver loads on its wings. At high dynamic pressures, the AAW control surfaces could be used as tabs that are deflected into the airstream to produce wing twists that minimize the control surface motion needed for aircraft maneuvering. Increased control effectiveness at high speeds is the main advantage of the AAW concept. The design of such an improved wing requires aeroservoelastic interaction studies between loads, unsteady aerodynamics, active controls, and structural aeroelasticity.

*Internship Student, Research Laboratory in Active Controls, Avionics and AeroServoElasticity, 1100 Notre Dame Street West; gabriel.kouba.1@ens.etsmtl.ca.

†Professor, Research Laboratory in Active Controls, Avionics and AeroServoElasticity, 1100 Notre Dame Street West; ruxandra@gpa.etsmtl.ca. Member AIAA.

‡Internship Student, Research Laboratory in Active Controls, Avionics and AeroServoElasticity, 1100 Notre Dame Street West; nicolas.boely.1@ens.etsmtl.ca.

The autoregressive moving-average and neural networks methods were used by Won et al. [4] to identify the flutter behavior of a transonic wing. Kukreja and Brenner [5] used the nonlinear autoregressive moving-average exogenous model for the flutter dynamics study of a pitch-plunge system subjected to limit cycle oscillations; Silva et al. [6], using the impulse response and the eigensystem realization algorithm methods, modeled the dynamics of a flexible wing model; and Le Garrec et al. [7] performed an output-error minimization method on a large flexible aircraft.

In F/A-18 aircraft flight flutter tests, the main structural and control surfaces considered are the left and right ailerons, the trailing-edge flaps, the rudders, the stabilizers, and the wings. Flutter excitations can be very dangerous for the stability and integrity of an aircraft and can possibly even lead to its complete destruction. Aircraft certification indeed requires that flutter vibrations be properly identified and controlled. In aerospace companies, flight-envelope limits calculated using finite element methods are verified and validated through flutter tests, and because of their complexity (aeroelastic and control knowledge), modern aeroservoelastic aircraft models may be identified by means of flutter tests. In fact, the F/A-18 aircraft model has already been identified and validated using the subspace method [8] from the same flight-test data.

Because the subspace method is a linearized method, we have chosen the nonlinear fuzzy logic identification method [9], which is more indicated for controller design than the subspace method. Indeed, linear methods degrade themselves in nonlinear control.

Furthermore, after more closely examining the fuzzy logic method, we realize that it is effective in decision-making [10,11]. The type of data NASA gave us needed reorganization, which was indeed permitted by this method. Indeed, the data could be ranged with a statistic approach [12]. This approach would permit a better control of those data [13].

For this work, only fuzzy logic is detailed because the neural network method was tested by another team. This team had the same purpose (the identification of the system [14]). After the reading of many documents, we concluded that the fuzzy logic and the neural network were two ways of describing and controlling a system [15]. Moreover, the two methods were already used in industry [16–18]. Previous research on the F/A-18 identification using neural network and fuzzy logic theories was performed by our team and presented in [19].

II. Methodology

A series of input and output data for 16 flight flutter test cases of a modified F/A-18 aircraft in the AAW program was determined by the NASA Dryden Flight Research Center laboratories. The tests were performed for 16 combinations of Mach numbers and altitudes. The F/A-18 aircraft outputs were given by the accelerations on the aircraft

surfaces, which were integrated twice in order to calculate the aircraft surface positions, and its inputs were given by onboard-excitation-system Shroeder excitations. The six inputs were for the left and right ailerons, the left and right rudders, and the left and right stabilizer positions, and the four outputs were given by the left and right wings and by the left and right trailing-edge flaps. For each of the 16 flutter test cases, an average of 15,000 points was recorded for each aircraft surface position or deflection variation in time. In order to best identify the F/A-18 aircraft from flight flutter tests, using the nonlinear fuzzy logic method, the following specifications or conditions were established for each 150 s flight test (the input's duration for NASA tests). The model time was not allowed to be longer than the actual time calculated during the flight. The specifications to be respected are that the fit coefficient must be greater than 98%, the robustness tests must be satisfied, and the simulation time must not exceed the 150 s recorded during flight flutter tests.

Two different fuzzy methods (Sugeno and Mandani) were tested in order to satisfy the above three conditions and specifications. This section is divided into three parts. In Sec. III, the two fuzzy logic methods are explained; we chose the Sugeno method because it offered a better performance. The model architecture is presented in Sec. IV by number of inputs and outputs, as well as by design. Sections IV.A–IV.C present the results obtained in terms of fit coefficients (first selection criterion), robustness, and the simulation times for different architectures, respectively. Section V presents the discussion and the model selection. Finally, conclusions and avenues for future work are presented.

III. Principles and Types of the Fuzzy Logic Method

A. Principle of the Method

The principles of the fuzzy logic method are described in [10], and Fig. 1 shows the system architecture created using the method.

Three main steps are involved in designing a system architecture using the fuzzy logic method. During the first step, the fuzzification section receives the input data x and transforms them into $F(x)$ by use of different membership functions. F could be linear, Gaussian, etc.
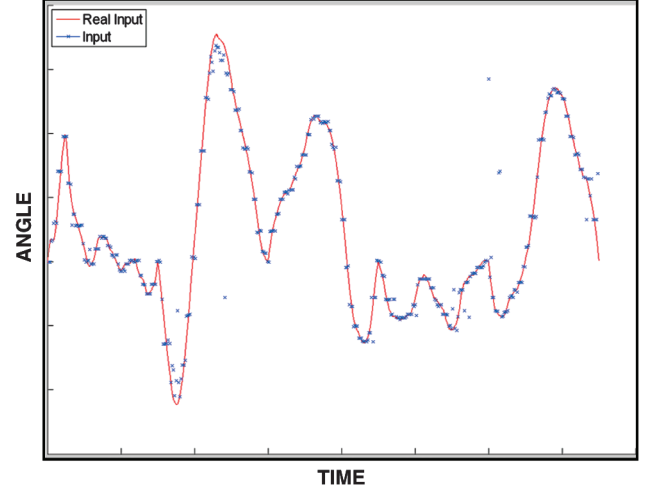

Fig. 3 Right wing model versus flight-test data output for the first flutter test case using the Mandani method.

We chose a Gaussian structure approach for the membership functions because it allows very good input or output data grouping for a statistical approach. Indeed, one of the main challenges in our work involved the management of a very large data set consisting of 15,000 points per flight case per input. Fuzzification allows the grouping of large data sets per membership, and the spectrum of all of the membership functions must describe all of the data sets.

In the next phase, called the inference phase, the input $F(x)$ is connected to the output $F'(y)$ by a series of rules. We already know which of the fuzzification memberships are connected with which defuzzification memberships or with one of the linear defuzzification combinations of memberships. Defuzzification memberships are calculated for the Mandani fuzzy-type method, and linear combination functions are calculated for the Sugeno fuzzy-type method. The output $F'(y)$ is obtained in fuzzy space from the inference block, and the desired output y is obtained from the defuzzification block. The
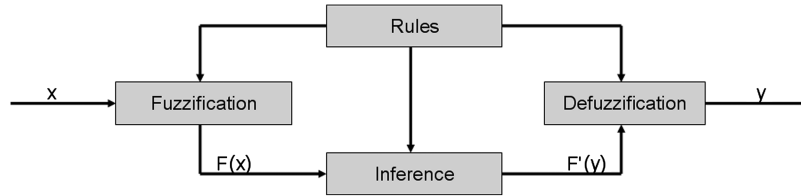

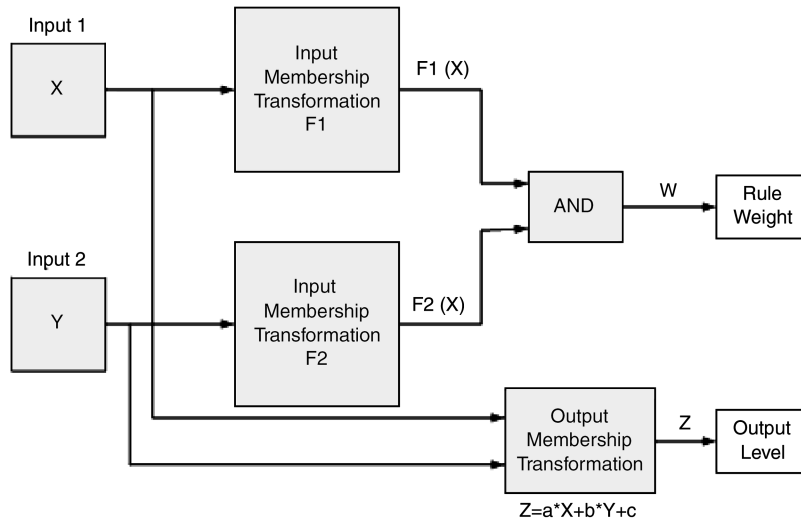**Fig. 1 System architecture created using the fuzzy logic method.**

Fig. 2 Operations required to obtain Z output level and W rule weights.

Table 1 Input-type systems (6, 12, 15, and 21) on the F/A-18 aircraft

Input abbreviations	Input names
lail, rail	Left and right aileron positions
lvert, rvert	Left and right rudder positions
lstb, rstb	Left and right stabilizer positions
deriv_lail, deriv_rail	Left and right aileron speeds
deriv_lvert, deriv_rvert	Left and right rudder speeds
deriv_lstb, deriv_rstb	Left and right stabilizer speeds
lail_lail, lstb_lstb, rstb_rstb, lvert_lvert, lail_lvert, lail_rvert, rail_lstb, lstb_lvert, lstb_rvert	Nine double products

Table 2 Summary of the different flight flutter test cases based on Mach numbers and altitudes

Flight condition	Mach number	Altitude 10^3 ft
1	0.85	5
2	0.85	10
3	0.85	15
4	0.9	5
5	0.9	10
6	0.9	15
7	1.1	10
8	1.1	15
9	1.1	20
10	1.1	25
11	1.2	10
12	1.2	15
13	1.2	20
14	1.2	25
15	1.3	20
16	1.3	25

differences between the two types of fuzzy logic methods are defined mainly in the defuzzification step.

B. Sugeno Method

For the Sugeno method [9], all of the input data are arranged in packages, with each grouping consisting of a range of values. To define the Gaussian memberships, we then determine the center of each package as well as its standard deviation. These Gaussian memberships will serve to transform x into $F(x)$ in the fuzzification step.

Following fuzzification, each output is a linear combination of fuzzy inputs. For example, after fuzzification, the two inputs x_1 and x_2 become x'_1 and x'_2, and the output can be written as $y = a_1 \times x'_1 + a_2 \times x'_2 + d_1$, where a_1, a_2, and d_1 are the polynomial coefficients.

Equations connecting the inputs x_j to the outputs y_i are written as follows:

$$Z_i = \sum_{j=1}^{n} A_{(i,j)}{}^* x_j + D_{(i,j)} \qquad (1)$$

where n is the number of inputs with $j \in [1, \ldots, n]$, A and D are the matrices containing the coefficients of the linear combinations between the fuzzy inputs and each output, x is the matrix containing the input data, and Z is considered as the output level $F'(y)$, as shown in Sec. III.A. The fuzzification part is executed by the F function:

$$W''_{(i,j)} = F_{(i,j)}(x_j) \qquad (2)$$

where

$$F_{(i,j)}(x_j) = \exp\left(-\sum_{i=1}^{N}\left(\frac{x_j - \mu_{(i,j)}}{\sqrt{2}^* \sigma_{(i,j)}}\right)^2\right)$$

$$W_i = \max\{W''_{(i,j)}\} \qquad (3)$$

where W_i is the matrix containing the weights of each data input, N is the number of rules with $i \in [1, \ldots, N]$, σ represents the standard deviations, and μ are the centers of packages. The y matrix containing the output data is defined in Eq. (4):

$$y = \frac{\sum_{i=1}^{N} W_i * Z_i}{\sum_{i=1}^{N} W_i} \qquad (4)$$

The F function serves to transform data inputs using the fuzzification step, in order to obtain the W weight matrix to be used in the y output calculation. This weight corresponds to the distance between the data input and the previously calculated Gaussian center.

The F fuzzification step, given by Eq. (2), is coupled to the W weight during the y output calculation, as indicated in Eq. (4).

The different operations that are required to obtain the Z output level, and the W rule weights are shown in Fig. 2.

C. Mandani Method

Much like with fuzzification, the Mandani-type method uses membership functions for defuzzification, and so we therefore composed an algorithm to compute a descriptive method in which each input is directly connected to its corresponding output. A fuzzy system was then created, containing one membership per data input and another per data output. This descriptive method has good potential, because in theory, it can be used to describe just about any system. However, after several tests, we realized that the resources involved would be huge, since we were unable to create systems with more than 125 points for each input using the MATLAB/Simulink software, and so we concluded that this method could not be efficient enough for the 15,000 points of our data set. However, the algorithm was found to be very good for systems with a small amount of data. Figure 3 shows the comparison between the right wing deflection model (shown in blue) and the right wing deflection flight-test data (shown in red) for the first flutter test case, realized using the Mandani method.

The fit coefficient for the curves shown in the figure was found to be smaller than 81.19%. The first specification was thus not satisfied even for this case, which was the best case as compared with other fit coefficients. Given the incompatibility of the Mandani method with our large data needs, as well as its comparatively low fit coefficient, we decided to use only the Sugeno method for our F/A-18 aircraft identification.

IV. Results

The Sugeno-type method was chosen, as was its architecture, described in Sec. III.B. Indeed, we realized after only a few tests that six inputs did not contain enough information to correctly complete the F/A-18 aircraft identification, and so we had to add more inputs in order to improve the values of the fit coefficients as well as the robustness of the test results.

Two additional input types were tested. We introduced, as shown in [8], the nine double products of the inputs, and we also decided to
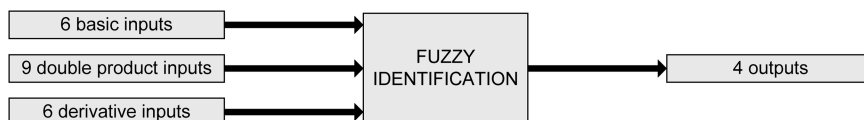
Fig. 4 F/A-18 aircraft system identification scheme with 21 inputs and four outputs represented in Simulink using the fuzzy identification scheme.

Table 3 Fit coefficients for the wings and flap deflection for all flight conditions for the 21-input system

Flight condition	Fit, % left wing	Fit, % right wing	Fit, % left trailing-edge flap	Fit, % right trailing-edge flap
1	99.49	99.61	99.68	99.7
2	99.85	99.92	99.79	99.85
3	99.71	99.72	99.8	99.83
4	99.66	99.87	99.87	99.73
5	99.79	99.88	99.58	99.67
6	99.75	99.87	99.54	99.81
7	99.68	99.87	99.68	99.77
8	99.84	99.9	99.66	99.9
9	99.54	99.68	99.9	99.89
10	99.86	99.9	99.53	99.71
11	99.92	99.92	99.93	99.92
12	99.68	99.82	99.81	99.67
13	99.82	99.91	99.87	99.86
14	99.86	99.86	99.73	99.77
15	99.88	99.91	99.94	99.82
16	99.66	99.79	99.74	99.91

Table 4 Fit coefficients for the wings and flap deflection for all flight conditions for the 12-input system

Flight condition	Fit, % left wing	Fit, % right wing	Fit, % left trailing-edge flap	Fit, % right trailing-edge flap
1	98.61	98.44	98.66	98.97
2	99.5	99.66	99.08	99.34
3	98.56	98.62	99.01	99.09
4	99.56	99.59	99.53	99.11
5	99.1	99.53	98.91	98.14
6	99.17	99.57	98.22	99.27
7	98.68	99.43	98.51	99.26
8	99.47	99.5	99.54	99.48
9	98.46	99.22	98.68	99.06
10	99.44	99.55	98.83	99.52
11	99.63	99.48	99.65	99.55
12	98.78	98.78	98.97	98.64
13	99.16	99.67	99.49	99.4
14	99.47	99.49	99.22	99.31
15	99.46	99.63	99.56	99.42
16	98.34	99.25	98.97	99.61

use the derivatives of each of the six inputs and therefore obtained a maximum of 21 inputs. Finally, four types of input combinations were chosen: the initial 6 inputs, the 12 inputs (the 6 inputs and their derivatives), the 15 inputs (the 6 inputs and their double products), and the 21 inputs (the 6 inputs, the 6 derivatives, and the 9 double products).

Fit coefficients were calculated for each of these four types of input combinations. When the fit coefficients did not have the desired high value, which is equivalent to not having the complete required specifications, the associated input combination was removed.

For a better visualization of the system physics, we enumerate the input-type systems (6, 12, 15, and 21) on the F/A-18 aircraft in Table 1.

The nine double products were chosen in previous work [8], where it was found that using all of them improved the precision of the system identification. The six derivatives were chosen because we needed to add more information to our aircraft system identification and because they are very important for aircraft identification from a physical point of view. A scheme of the system is shown in Fig. 4, in which the maximum number of inputs (21) is considered.

A. Fit Coefficient Analysis

In this section, we validate which of the four input combinations would give the best output combination to fit actual flight-test data outputs. Out of the four input combinations, both the 6- and 15-input systems were removed from further consideration, because their fit

coefficients were lower than 95%. The two other input systems with 12 and 21 inputs gave much better results and are shown below.

The F/A-18 aircraft flight flutter test cases are given for 16 different combinations of Mach numbers and altitudes, as illustrated in Table 2.

For each flight condition, Tables 3 and 4 summarize the fit coefficients for the model identification and validation for the 21- and the 12-input systems, respectively. The minimum fit-coefficient values are highlighted in red, and the maximum fit-coefficient values are highlighted in green.
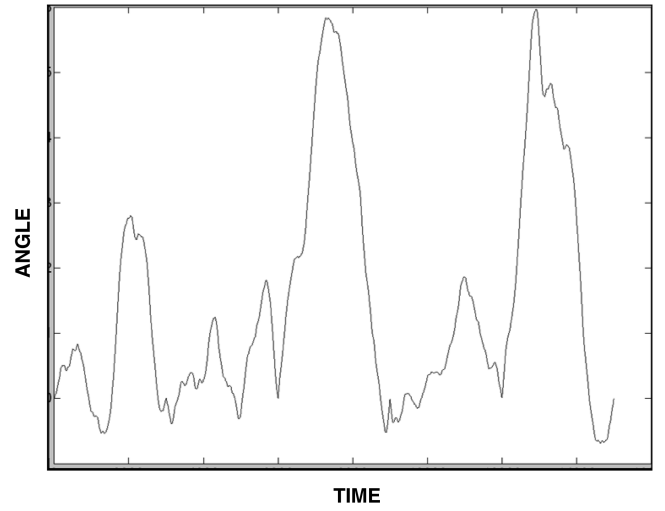
B. Robustness Test

For the robustness tests, here we show only the results for the first flight-test case, while pointing out that those obtained for the other flight cases are similar. Different numbers were considered for the input points instead of the initial 15,000 points, and then a linear interpolation was performed between these points before they were input into the model. For example, we took the first and the fifth input points and then calculated the three points between by tracing a line. The fit coefficients were then calculated for each set of input data numbers, and the maximum and the minimum fit coefficients are presented here for the first flight case.

In Figs. 5a–5d, the time variation for the left wing input (lwing) for the first flight case is given for various sets of data input according to the number of points we took. The purpose was to demonstrate the linearization between the remaining points. In Fig. 5a, all of the input points are considered (15,000 points on 15,000). In Fig. 5b, one out
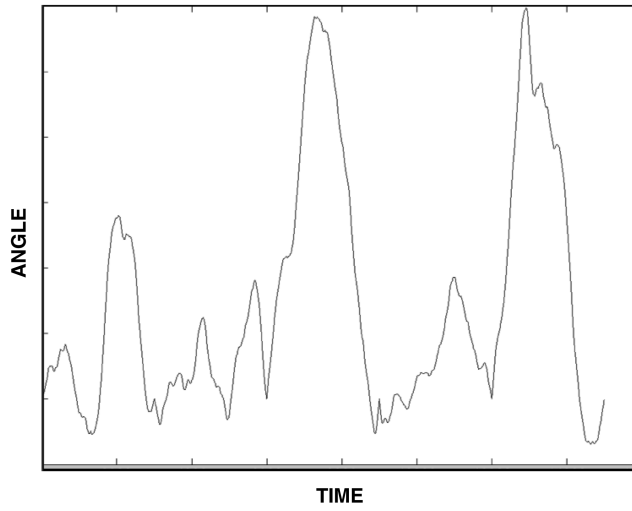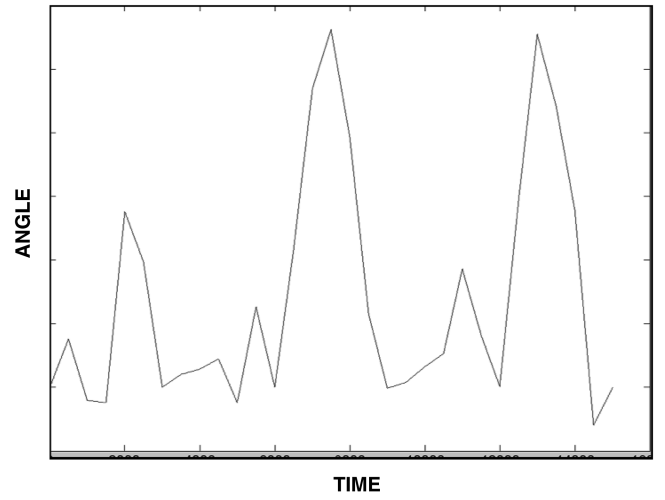
a) All input points

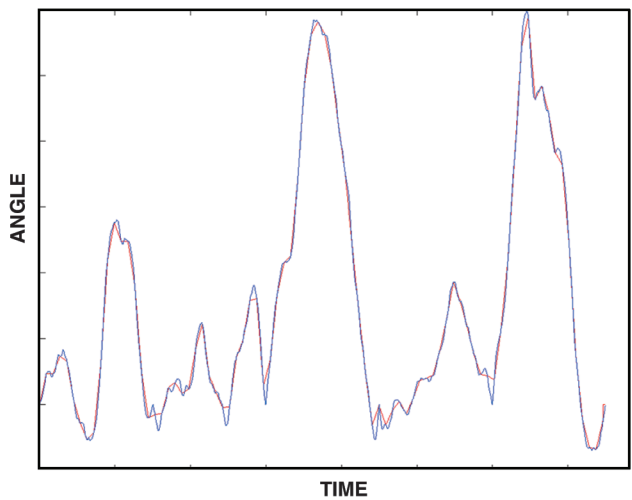b) One out of 100 input points
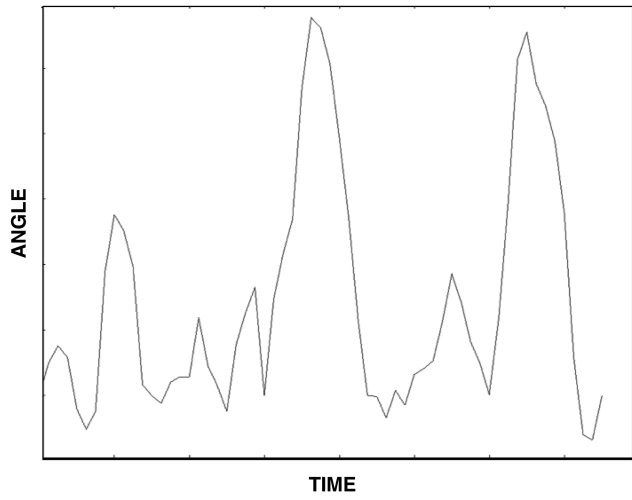
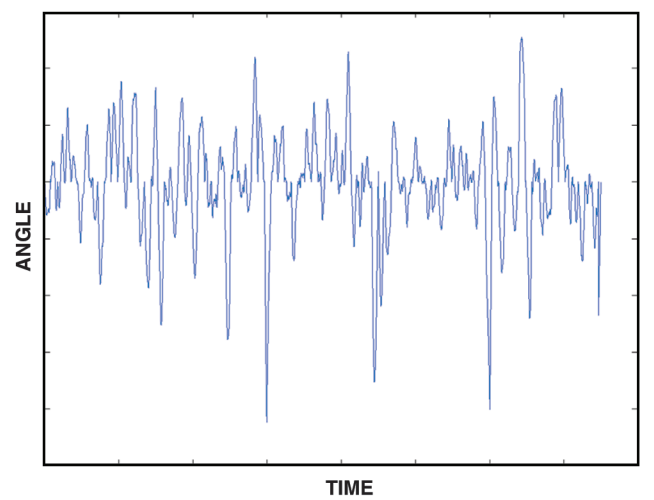

c) One out of 250 input points

d) One out of 500 input points

Fig. 5   Comparison between four different sets of data input for the robustness test.

a) Comparison between results obtained with all input data (in red) and results obtained with one out of 180 input points (in blue) for the first flight case

b) Errors between results obtained with all input data and results obtained with one point out of 180 input points for the first flight case

Fig. 6   Comparison between the real set of data and a robustness set of data.

Table 5 Numerical values of minimum and maximum fit coefficients for the 21-input system

| Number of points	FITMIN, %	FITMAX, %
15,000	99.4925	99.7045
7,500	99.4654	99.7023
3,000	99.4694	99.6985
1,500	99.4488	99.6926
300	98.3674	99.2272
150	95.8845	98.1071
115	92.5732	96.7676
100	90.74	93.9833
83	83.8159	94.3118
75	66.1333	85.8318
60	65.2642	82.6349
30	16.4895	43.1858
20	5.0484	22.5459

Table 6 Numerical values of minimum and maximum fit coefficients for the 12-input system

Number of points	FITMIN, %	FITMAX, %
15,000	98.4384	98.9728
7,500	98.5017	99.0103
3,000	97.7356	98.8727
1,500	97.775	98.9362
300	97.4888	98.6438
150	96.2249	97.5319
115	95.0173	96.8294
100	93.9231	95.939
83	91.4686	94.7172
75	90.1286	94.8377
60	89.5585	93.5961
30	69.9965	82.154
20	45.6167	72.5392

of 100 input points is considered (150 points on 15,000); in Fig. 5c, one out of 250 input points is considered (60 points on 15,000); and in Fig. 5d, one out of 500 input points is considered (30 points on 15,000). Those four figures compare the differences between the choice of the number of points taken.

Following an analysis of Figs. 5a–5d, a comparison is shown in Fig. 6a between the results obtained with all of the flight-test input data, represented in red, against those obtained with one set of one out of 180 input points, which are highlighted in blue. In fact, we have chosen the 180-input data case as the best input data combination. The error, represented as the difference between these results, is shown in Fig. 6b.

The errors between the two sets of results extend only to very small values, such as 0.4°, and the effects of such errors on the fit-coefficient values are studied for the 12-input and 21-input systems. We chose to study the effects of the minimum and maximum fit
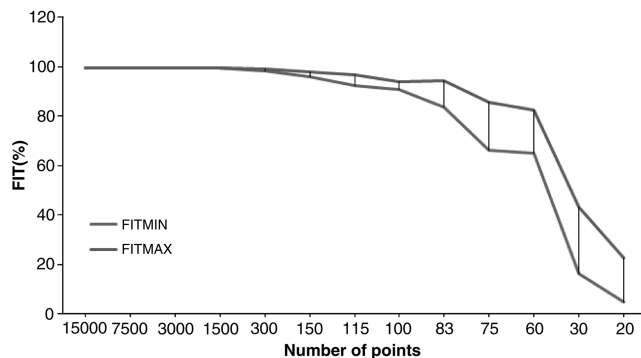
Fig. 7 Extreme fit-coefficient values (minimum and maximum) for the 21-input system.
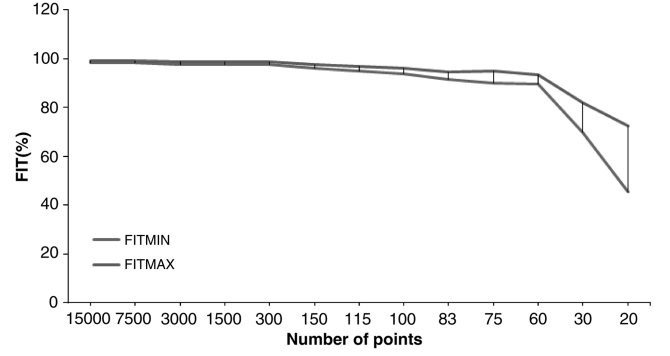
Fig. 8 Extreme fit-coefficient values (minimum and maximum) for the 12-input system.

coefficients, abbreviated as FITMIN and FITMAX in both the 21- and the 12-input data systems. Numerical values of FITMIN and FITMAX are given in Tables 5 and 6 for the 21- and for the 12-input systems, respectively. The same values are represented in a visual form in Figs. 7 and 8 for the 21- and the 12-input systems, respectively.

C. Time Simulation

Here, we show the time simulation for the four systems (i.e., with 6, 12, 15, and 21 data inputs). The results for an average over 10 simulations of 150 s ($150 \times 10 = 1500$ s) are shown numerically in Table 7 for each of the four input combinations. The goal here is to quantify the differences between computer execution speeds for the four different data input systems. Those results are also shown in Fig. 9.

V. Results Interpretation

A. Discussion

The Mandani system was designed for minor systems, and was quickly abandoned because of its poor performance on bigger systems. It was unable to group data together into statistic clusters, and the algorithm was not optimized, as shown in Fig. 3.

As shown in Tables 3 and 4, both Sugeno systems presented met the first type of specification very well, in terms of fit-coefficient values. A quick observation reveals that the 21-input system gave slightly better fits than did the 12-input system. Because the differences in the fit-coefficient values were very small, it was still necessary to perform additional work on the systems' robustness and on their time-simulation capacities in order to decide which of these two input systems would offer a better performance.

From Tables 5 and 6, resuming the robustness test, it is clear that the number of points required to obtain a fit coefficient higher than 80% is 83 points for the 21-input data system and only 60 for the 12-input data system. Therefore, we concluded that the 12-input system is more robust from the perspective of this second selection criterion.

It is known that one perturbation induced in the six initial inputs will influence all of the other built inputs (nine input products and six derivatives). Specifically, for the 12-input system, the error will

Table 7 Computer execution simulation time for four different input-data-combination systems

Type of system (input combinations)	Computer execution simulation time, s[a]
6-input	3.93
12-input	45.33
15-input	6.25
21-input	90.55

[a]Expressed as an average over 10 simulations.
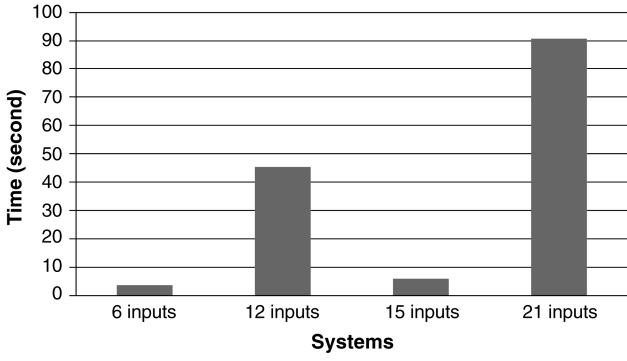
Fig. 9   Simulation times for the four systems obtained with different combinations of input data.

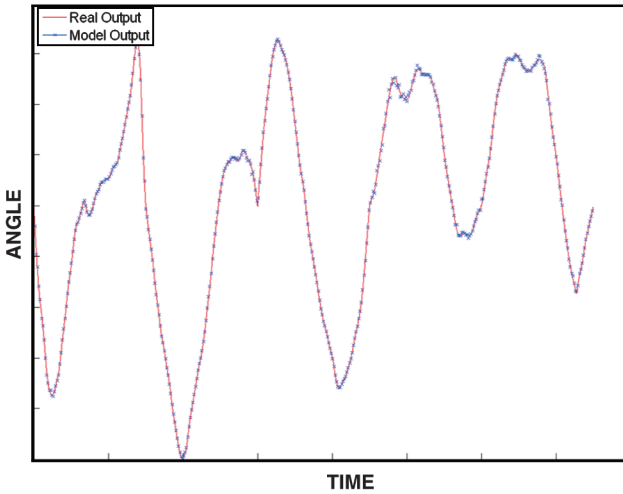21 inputs, the execution time increases because of the Simulink resources involved.

B.   System Choice

From the four data-input-combination systems, we chose the 12-input system as the one that best satisfies each of the project's specifications:
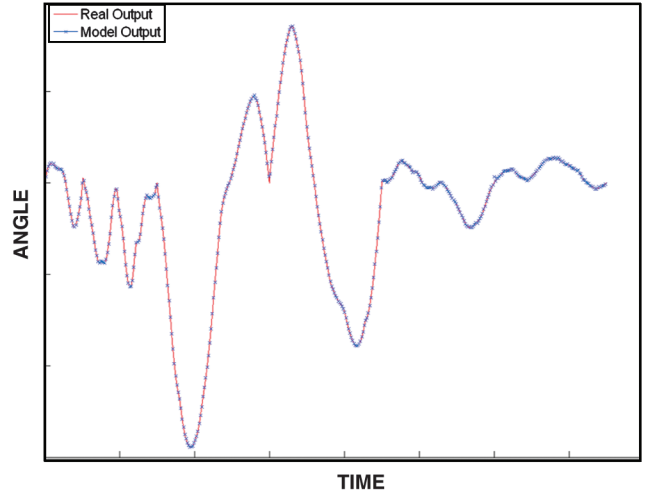
1) The fit coefficients are all higher than 98%.

2) The system is robust, as it can be identified with one out of 50 input points and still have a fit coefficient higher than 97%.

3) A computer simulation time average of 45 s is obtained, which is significantly less than 150 s.

In Figs. 10a–10d, the fuzzy-model curve outputs (blue) are shown in comparison to the flight-test curve-data outputs (red) for the flight-test case no. 7, which represent flight at a Mach number equal to 1.1 and at an altitude equal to 10,000 ft. In those figures, these types of results are shown for the following aircraft surfaces: Fig. 10a shows the left wing (lwing), Fig. 10b shows the right wing (rwing), Fig. 10c shows the left trailing-edge flaps (ltef), and Fig. 10d shows the right trailing-edge flaps (rtef).
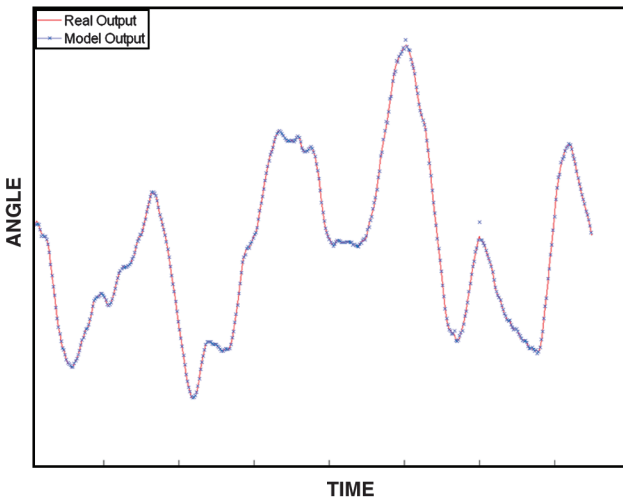
Figures 11a and 11b show the robustness test results for flight-test case 1, which represent the flight at a Mach number equal to 1.1 and at an altitude equal to 10,000 ft. Out of the four output results, only two output results are represented: the one with the best fit coefficients for the rtef (Fig. 11a) and the one with the worst fit coefficients for the lwing (Fig. 11b). The fuzzy-model curve outputs are given in blue points, and the flight-test curve data are shown as red curves.
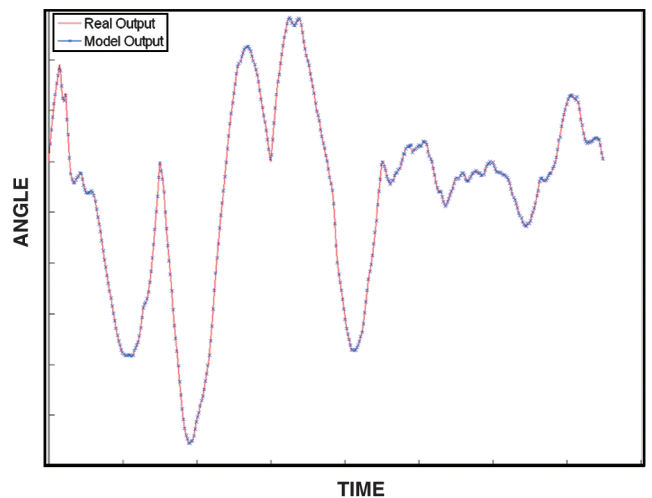
influence only the input derivatives, and for the 21 inputs, the error will also influence their products and thus induce a greater number of perturbations. Therefore, the fit-coefficient values will degrade faster for the 21-input system, as verified by robustness studies.

From Table 7, we can see that all simulation times are less than 150 s, and so the third specification mentioned in Sec. II is therefore satisfied. Still from Table 7, it can be observed that the 21-input system requires twice as much computer execution time (90 s) as the 12-input system (45 s), which can be explained by the fact that when derivatives are added to the given inputs in order to obtain the 12 and

a) Left wing deflection

b) Right wing deflection

c) Left trailing edge flap deflection

d) Right trailing edge flap deflection

Fig. 10   Comparison of the output data between flight test (red curve) and model simulation (blue points).

a) Comparison of the flight test data with model data for the
right trailing edge flaps

b) Comparison of the flight test data and model data for the
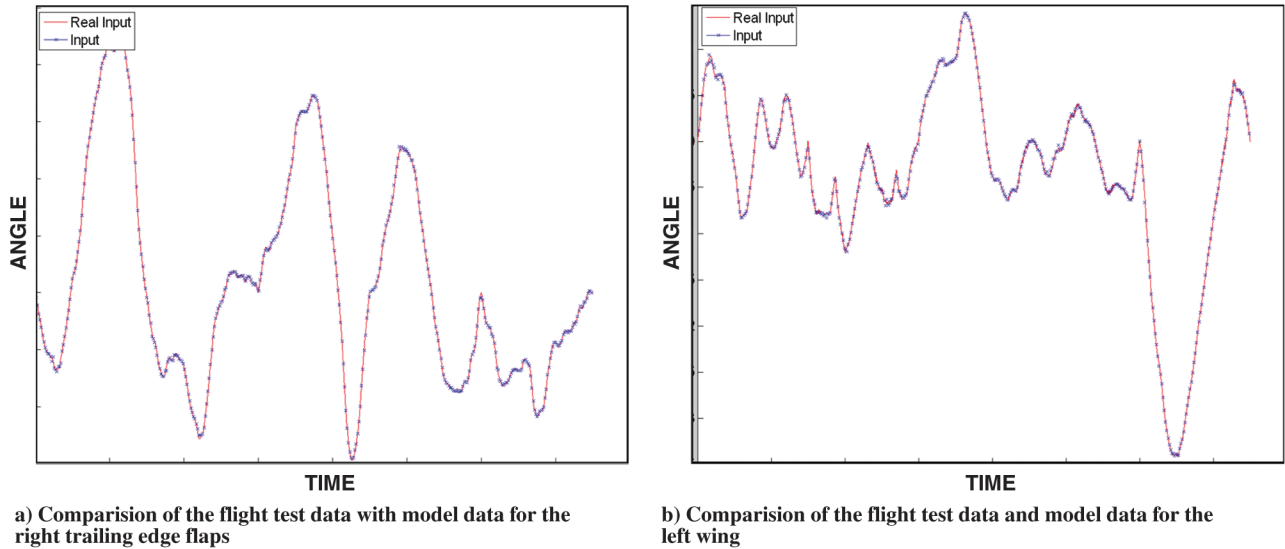left wing

Fig. 11   Curves of the robustness test for 300 input points instead of all 15,000 points.

VI.   Conclusions

Modeling the aircraft using a fuzzy model has allowed us to describe flutters observed on computer simulations. The cost of actual flights and for the collection of such data can be high, and so modeling such systems is a great first step to understanding them. Once models are calculated, we can work on them to introduce new principles in order to directly observe the plane's responses.

In the near future, using the identified and validated model created here, a closed-loop controller will be conceived in which the desired output will be considered as its input. Other future applications could be derived from these types of identification and validation studies. For example, we could suppress the flutter phenomenon during critical flight phases or induce flutter on certain aircraft surfaces in order to control aircraft motion, thus improving stability and performance.

Acknowledgments

References

[1] Voracek, D., Pendleton, E., Reichenback, E., Griffin, K., and Welch, L., "The Active Aeroelastic Wing Phase I Flight Research Through January 2003," NASA TM-2003-210741, April 2003.

[2] Lee, D., Baldeli, D., Lindsley, N., and Brenner, M., "Static Aeroelastic and Open-Loop Aeroservoelastic Analyses for the F/A-18 AAW Aircraft," AIAA Paper 2007-2135, April 2007.

[3] Pendleton, E., Flick, P., Paul, D., Voracek, D., Reichenbach, E., and Griffin, K., "The X- 53, A Summary of the Active Aeroelastic Wing Flight Research Program," AIAA Paper 2007-1855, April 2007.

[4] Won, K., Tsai, H., Sadeghi, M., and, Liu, F., "Non-Linear Impulse Methods for Aeroelastic Simulations," AIAA Paper 2005-4845, June 2005.

[5] Kukreja, S. L., and Brenner, M., "Nonlinear Aeroelastic System Identification with Application to Experimental Data," *Journal of Guidance, Control, and Dynamics*, Vol. 29, No. 2, 2006, pp. 374–381.
doi:10.2514/1.15178

[6] Silva, W. A., Vartio, E., Shimko, A., Segundo, E. I, Kvaternik, R. G., Eure, K. W., and Scott, R., "Development of Aeroservoelastic Analytical Models and Gust Load Alleviation Control Laws of a Sensorcraft Wind-Tunnel Model Using Measured Data," AIAA Paper 2006-1935, May 2006.

[7] Le Garrec, C., Humbert, M., Bucharles, A., and Vacher, P., "In-Flight Aeroelastic Model Identification and Tuning of a Flight Control System on a Large Civil Aircraft," *IFASD: International Forum on Aeroelasticity and Structural Dynamics* [CD-ROM], Madrid, 5–7 June 2001.

[8] De Jesus Mota, S., Nadeau Beaulieu, M., Botez, R. M., and Brenner, M., "Modeling of Structural Deflections on an F/A-18 Aircraft Following Flight Flutter Tests by Use of the Subspace Method," AIAA Paper 2007-6303, Aug. 2007.

[9] Passino, K. M., and Yurkovich, S., *Fuzzy Control*, Addison-Wesley-Longman, Menlo Park, CA, 1998.

[10] Mondani, E. H., "Applications of Fuzzy Logic to Approximate Reasoning Using Linguistic Synthesis," *IEEE Transactions on Computers*, Vol. 26, No. 12, Dec. 1977, pp. 1182–1191.
doi:10.1109/TC.1977.1674779

[11] Zadeh, L., "Fuzzy Logic," *Computer*, Vol. 21, No. 4, April 1988, pp. 83–93.
doi:10.1109/2.53

[12] Kosko, B., "Fuzziness vs. Probability," *International Journal of General Systems*, Vol. 17, No. 2, 1990, pp. 211–240.

[13] Zadeh, L. A., "Fuzzy Sets," *Information and Control*, Vol. 8, 1965, pp. 338–353.
doi:10.1016/S0019-9958(65)90241-X

[14] Chen, S., and Billings, S. A., "Neural Networks for Nonlinear Dynamic System Modeling and Identification," *International Journal of Control*, Vol. 56, No. 2, 1992, pp. 319–346.
doi:10.1080/00207179208934317

[15] Hunt, K. J., and Sbarbaro, D., "Neural Networks for Nonlinear Internal Model Control," *IEE Proc-D, Control Theory and Applications*, Vol. 138, No. 5, Sept. 1991, pp. 431–438.

[16] Sugeno, M., *Industrial Application of Fuzzy Control*, Elsevier Science, New York, 1985.

[17] Hunt, K. J., Sbarbaro, D., Zbikowski, R., and Gawthrop, P. J., "Neural Networks for Control Systems-A Survey," *Automatica*, Vol. 28, No. 6, Nov. 1992, pp. 1083–1112.
doi:10.1016/0005-1098(92)90053-I

[18] Narendra, K. S., Parthasarathy, K, "Identification and Control of Dynamical Systems Using Neural Networks," *IEEE Transactions on Neural Networks*, Vol. 1, No. 1, March 1990, pp. 4–27.
doi:10.1109/72.80202

[19] Boely, N., Botez, R., and Kouba, G., "Identification of An F/A-18 Nonlinear Model Between Control and Structural Deflections," AIAA Paper 2009-426, Jan. 2009.